International Journal of Modern Physics B
Vol. 30 (2016) 1650122 (11 pages)

DOI: 10.1142/S0217979216501228

Conduction band population in graphene in ultrashort strong laser field: Case of massive Dirac particles

Z. Ahmadi, H. Goudarzi* and A. Jafari†
Department of Physics, Faculty of Science, Urmia University, P. O. Box 165, Urmia, Iran
**h.goudarzi@urmia.ac.ir*
†*a.jafari@urmia.ac.ir*

Received 16 December 2015
Revised 3 March 2016
Accepted 11 March 2016
Published 10 May 2016

The Dirac-like quasiparticles in honeycomb graphene lattice are taken to possess a non-zero effective mass. The charge carriers involve to interact with a femtosecond strong laser pulse. Due to the scattering time of electrons in graphene ($\tau \approx 10$–100 fs), the one femtosecond optical pulse is used to establish the coherence effect and, consequently, it can be realized to use the time-dependent Schrödinger equation for electron coupled with strong electromagnetic field. Generalized wave vector of relativistic electrons interacting with electric field of laser pulse causes to obtain a time-dependent electric dipole matrix element. Using the coupled differential equations of a two-state system of graphene, the density of probability of population transition between valence (VB) and conduction bands (CB) of gapped graphene is calculated. In particular, the effect of bandgap energy on dipole matrix elements at the Dirac points and resulting CB population (CBP) is investigated. The irreversible electron dynamics is achieved when the optical pulse end. Increasing the energy gap of graphene results in decreasing the maximum CBP.

Keywords: Gapped graphene; femtosecond laser pulse; dipole matrix element; conduction band population.

PACS numbers: 72.80.Vp, 73.22.Pr, 78.47.J−

1. Introduction

Two-dimensional honeycomb atomic lattice of graphene[1,2] demonstrates a potential of great prosperity within several applications due to its peculiar electronic, optical and mechanical properties.[3–6] The electron dynamics in pristine graphene obeys the massless relativistic Dirac equation and low-energy dispersion has a linear dependence on momentum in the first Brillouin zone. There are two degenerate

*Corresponding author.

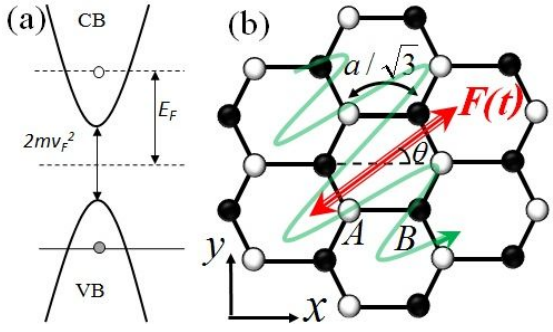

Fig. 1. (Color online) (a) Opening bandgap $E_g = 2mv_F^2$ in energy dispersion of graphene near the Dirac points in reciprocal space and level of Fermi energy E_F, VB and CB correspond to valence and conduction band, respectively, and (b) sketch of lattice structure of graphene which is illuminated by laser pulse. A and B correspond to two inequivalent sublattices. Optical pulse is perpendicularly glinted to the graphene sheet and its electric field makes angle θ with x-direction in graphene plane.

inequivalent valleys, locating at the corners of the Brillouin zone (K and K' Dirac points), which the valence (VB) and conduction bands (CB) of two sublattices A and B relating to the pseudospin cross at the Dirac points. Indeed, the pristine graphene is considered as a semiconductor with zero bandgap. Actually, this is considered as a restriction for many optical and electronics applications. However, inducing a bandgap to graphene can be achieved by several methods,[7–16] for instance, in graphene grown on SiC-substrate,[8,9] and, dynamically important, by endurance of uniaxial mechanical strain up to 22%.[16] Thus, one can expect that the massive Dirac-like electrons demonstrate a fundamentally distinct dynamical and transport behavior.

In the last few years, interaction of external electromagnetic fields with condensed matters has attracted several theoretical and experimental researches.[17–23] Thereby, a high intensity optical pulse can strongly affect the electron dynamics and, correspondingly, modify the transport and optical properties.[24,25] The reversibility of electron dynamics in insulators in the presence of a laser field, after the pulse end has been investigated.[26] Interaction of electrons in metals with a strong optical pulse gives rise to a high frequency Bloch oscillation.[27] It is observed that a distinct behavior for charge carrier dynamics in graphene interacting with ultrafast (one optical oscillation) and strong ($\approx 1\ V/\text{Å}$) optical pulse, comparing with both insulators and metals,[28] where the authors have shown that the dynamics of quasiparticles in pristine graphene with a laser pulse is not reversible when the laser pulse is over, and a large residual CB population (CBP) is obtained.

In this paper, we investigate the effect of massive Dirac fermions on the interband transition in a gapped graphene interacting with an ultrashort laser pulse. We focus on the interband mixing of the VB and CB separated from each other by a $2mv_F^2$ energy gap. A schematic of Dirac point with an energy gap between CB and VB is sketched in Fig. 1(a). The wave vector of charge carriers is modified by

the time-dependent vector potential of laser pulse, while the electric field causes to create an electric dipole moment between the states of the CB and VB. Influence of an energy gap between CB and VB can significantly affect mentioned dipole moments, since the excitation of electrons may be a nonzero value at the Dirac points.

This paper is organized as follows. In Sec. 2, we present the proposed structure and related formalism to obtain the explicit form of dipole matrix elements and exact relation for time-dependent CBP. The numerical results and discussion about the influence of energy gap between CB and VB of graphene in the dynamics of quasiparticles are presented in Sec. 3. Finally, we summarize our findings in Sec. 4.

2. Model and Formalism

This section follows closely the presentation of the methodology described in Ref. 28. In order to study the effect of population transition between VB and CB in gapped graphene illuminated by ultrafast laser field, we consider an optical laser pulse that is normally incident on a graphene sheet with linear polarization in graphene plane, as shown in Fig. 1(b). The gapped graphene Hamiltonian H_0 is introduced within the nearest-neighbor tight-binding model[29] by a 2×2 matrix of the form:

$$H_0 = \begin{pmatrix} \alpha - E_{\mathrm{F}} & \gamma f(\mathbf{k}) \\ \gamma f^*(\mathbf{k}) & -\alpha - E_{\mathrm{F}} \end{pmatrix}, \tag{1}$$

where $\gamma = -3.03$ eV and E_{F} are the hopping integral and Fermi energy, respectively. $\alpha = m\sigma_z$ denotes bandgap of graphene, where m is the effective mass of Dirac fermions and σ_z is the Pauli matrix. The off-diagonal term of Hamiltonian is given by

$$f(\mathbf{k}) = \exp\left(\frac{iak_x}{\sqrt{3}}\right) + 2\exp\left(\frac{-iak_x}{2\sqrt{3}}\right)\cos\left(\frac{ak_y}{2}\right) = |f(\mathbf{k})|e^{i\varphi_k}\,, \tag{2}$$

where $a = 2.46$ Å is lattice constant and $\mathbf{k}$ denotes the wave vector of electron. The energy spectrum of Hamiltonian H_0 consist of the CB (π^*) and the VB (π) with the energy dispersion $\epsilon_{c,v} = \pm\sqrt{m^2 + \gamma^2|f(\mathbf{k})|^2} - E_{\mathrm{F}}$. By solving the Dirac equation for Hamiltonian Eq. (1), the corresponding wavefunctions are given as

$$\psi_{\mathbf{k}}^{(c)}(\mathbf{r}) = \frac{e^{i\mathbf{k}\cdot\mathbf{r}}}{\sqrt{2}} \begin{pmatrix} \sqrt{\dfrac{\epsilon_c + E_{\mathrm{F}} + m}{\epsilon_c + E_{\mathrm{F}}}}\, e^{i\varphi_k} \\ \sqrt{\dfrac{\epsilon_c + E_{\mathrm{F}} - m}{\epsilon_c + E_{\mathrm{F}}}} \end{pmatrix}, \tag{3}$$

$$\psi_{\mathbf{k}}^{(v)}(\mathbf{r}) = \frac{e^{i\mathbf{k}\cdot\mathbf{r}}}{\sqrt{2}} \begin{pmatrix} -\sqrt{\dfrac{\epsilon_c + E_{\mathrm{F}} - m}{\epsilon_c + E_{\mathrm{F}}}}\, e^{i\varphi_k} \\ \sqrt{\dfrac{\epsilon_c + E_{\mathrm{F}} + m}{\epsilon_c + E_{\mathrm{F}}}} \end{pmatrix}, \tag{4}$$

where two components of wavefunctions belong to the sublattices A and B, respectively, as shown in Fig. 1(a). Opening a bandgap in graphene does not change the linearity of energy dispersion near the Dirac points and the band structure of the doped graphene is similar to the band structure of pristine graphene. However, existence of bandgap can be an important feature for electronics and optical applications, and actually, gives rise to a new behavior of relativistic quasiparticles in transitions between distinct bands. Normally incident optical pulse on a gapped graphene sheet is taken to be

$$F(t) = F_0 e^{-u^2}(1 - 2u^2)\,. \tag{5}$$

This form of optical pulse is an idealization of the actual 1.5 oscillation pulses used in recent experiments.[24,25] F_0 is the amplitude of pulse, $u = t/\tau$ and τ denotes the pulse length, which is set $\tau = 1$ fs corresponding to carrier frequency $\omega = 1.5\ \mathrm{eV}/\hbar$. We suppose the pulse is linearly polarized, so that the plane of polarization is characterized by angle θ measured relative to x-axis [see Fig. 1(b)]. The electrons in gapped graphene may interact with a time-dependent electric field of optical pulse, in which its Hamiltonian reads:

$$\mathcal{H}(t) = H_0 + e\mathbf{F}(t)\cdot\mathbf{r}\,, \tag{6}$$

where $\mathbf{r}$ is a two-dimensional space vector. If the length of pulse is less than the characteristic time of electron scattering, which is 10–100 fs[30–35] then the electron dynamics in external electric field may be coherent, and consequently, it is described by the time-dependent Schrödinger equation.

The electric field of optical pulse accelerates the electrons of graphene in the direction of the field polarization through the graphene plane, and also changes the wave vector $\mathbf{k}$ of electrons. Moreover, the electric field can affect both intraband and interband electron dynamics. The interband electron dynamics gives rise to coupling the CB and VB states, and makes a redistribution of electrons between two bands. First, we describe the electron dynamics within a single band in the reciprocal space, which is determined by acceleration theorem

$$\hbar\frac{d\mathbf{k}(t)}{dt} = e\mathbf{F}(t)\,. \tag{7}$$

For an electron with initial momentum $\mathbf{q}$ at the first Brillouin zone in corners of honeycomb lattice, one can obtain the generalized time-dependent wave vector $\mathbf{k}(\mathbf{q}, t)$ as

$$\mathbf{k}(\mathbf{q}, t) = \mathbf{q} + \frac{e}{\hbar}\int_{-\infty}^{t}\mathbf{F}(t_1)dt_1 \tag{8}$$

and corresponding wavefunction can be expressed as Houston functions,[36]

$$\Phi^{(H)}_{\delta\mathbf{q}}(\mathbf{r}, t) = \psi^{(\delta)}_{\mathbf{k}(\mathbf{q},t)}(\mathbf{r})\exp\left(\frac{-i}{\hbar}\int_{-\infty}^{t} dt_1\,\epsilon_\delta[\mathbf{k}(\mathbf{q}, t_1)]\right), \tag{9}$$

where $\psi^{(\delta)}_{\mathbf{k}(\mathbf{q},t)}(\mathbf{r})$ is the Dirac spinor of Eqs. (3) and (4). Finally, solving the Schrödinger equation for interacting Hamiltonian $\mathcal{H}(t)$ is given by the superposition of Houston functions:

$$\Psi_{\mathbf{q}}(\mathbf{r},t) = \sum_{\delta=c,v} \beta_{\delta\mathbf{q}}(t)\Phi^{(H)}_{\delta\mathbf{q}}(\mathbf{r},t)\,, \tag{10}$$

where $\beta_{\delta\mathbf{q}}(t)$ is corresponding time-dependent expansion coefficients. Due to the acceleration theorem, the electrons which belong to the different bands but have the same initial wave vector $\mathbf{q}$ possesses the same wave vector $\mathbf{k}(\mathbf{q},t)$ at later moment of time t. Coupling of CB and VB states in external electric field is determined by an interband dipole matrix element. The interband dipole matrix element is diagonal in reciprocal space, so the states with different wave vector are not coupled by the pulse field. Such coupling of states with the same value of $\mathbf{q}$ is the property of the coherent dynamics. Substituting wavefunctions expressed in Eq. (10) into the time-dependent Schrödinger equation results in two coupled differential equations

$$\begin{aligned}
\frac{d\beta_{c\mathbf{q}}(t)}{dt} &= \frac{-i}{\hbar}\mathbf{F}(t)\cdot\mathbf{Q}_{\mathbf{q}}(t)\beta_{v\mathbf{q}}(t)\,,\\
\frac{d\beta_{v\mathbf{q}}(t)}{dt} &= \frac{-i}{\hbar}\mathbf{F}(t)\cdot\mathbf{Q}^{*}_{\mathbf{q}}(t)\beta_{c\mathbf{q}}(t)\,,
\end{aligned} \tag{11}$$

in which one can easily obtain the interband dipole matrix element $\mathbf{Q}_{\mathbf{q}}(t)$ as

$$\mathbf{Q}_{\mathbf{q}}(t) = \mathbf{D}[\mathbf{k}(\mathbf{q},t)]\exp\left\{\frac{-i}{\hbar}\int_{-\infty}^{t} dt_1[\epsilon_c[\mathbf{k}(\mathbf{q},t_1)] - \epsilon_v[\mathbf{k}(\mathbf{q},t_1)]]\right\}, \tag{12}$$

where $\mathbf{D}(\mathbf{k}) = \langle\psi^{(c)}_{\mathbf{k}}|e\mathbf{r}|\psi^{(v)}_{\mathbf{k}}\rangle$ is the dipole matrix element between distinct bands with wave vector $\mathbf{k}$. By substituting Eqs. (3) and (4) into the expression $\mathbf{D}(\mathbf{k})$, we can obtain the following expressions for the interband dipole matrix elements as follows:

$$D_j(\mathbf{k}) = \sqrt{1-\left(\frac{m}{\epsilon_c+E_{\mathrm{F}}}\right)^2}Z_j - \frac{ie}{2}\frac{m\partial\epsilon_c/\partial k_j}{(\epsilon_c+E_{\mathrm{F}})\sqrt{(\epsilon_c+E_{\mathrm{F}})^2-m^2}}\,;\quad (j=x,y)\,, \tag{13}$$

where we have defined

$$Z_x = \frac{ea}{2\sqrt{3}}\frac{1+\cos\left(\frac{ak_y}{2}\right)\left[\cos\left(\frac{3ak_x}{2\sqrt{3}}\right)-2\cos\left(\frac{ak_y}{2}\right)\right]}{1+4\cos\left(\frac{ak_y}{2}\right)\left[\cos\left(\frac{3ak_x}{2\sqrt{3}}\right)+\cos\left(\frac{ak_y}{2}\right)\right]}\,,$$

$$Z_y = \frac{ea}{2}\frac{\sin\left(\frac{ak_y}{2}\right)\sin\left(\frac{3ak_x}{2\sqrt{3}}\right)}{1+4\cos\left(\frac{ak_y}{2}\right)\left[\cos\left(\frac{3ak_x}{2\sqrt{3}}\right)+\cos\left(\frac{ak_y}{2}\right)\right]}\,.$$

If the energy gap is taken to be zero, then dipole matrix element reduces to that which has been obtained in Ref. 28. For solving the coupled differential equations of two-state system of Eq. (11) which describes the interband electron dynamics and, indeed, determines the mixing of the states in the presence of electric field of laser pulse, we consider the initial condition as $(\beta_{v\mathbf{q}}, \beta_{c\mathbf{q}}) = (1, 0)$, which denotes the condition before interaction of electric field of the pulse with quasiparticles in the gapped graphene. All the states of VB are occupied, and consequently, the states of CB are empty. The mixing of the states from different bands and the dynamics of an electron which initially lies in the VB is characterized by the time-dependent expansion coefficients $|\beta_{c\mathbf{q}}(t)|^2$. The time-dependent total transition of CB is expressed by the following expression:

$$N_{\mathrm{CB}}(t) = \sum_{\mathbf{q}} |\beta_{c\mathbf{q}}(t)|^2 , \tag{14}$$

where the sum is over all momentum in the first Brillouin zone.

3. Numerical Results and Discussion

In this section, we discuss, in detail, about the CBP, resulting from Eq. (14) with respect to the bandgap energy of graphene. Very recently in Ref. 28, the authors have stated that the gapless energy dispersion of pristine graphene is responsible to the irreversible electron dynamics in an optical field. Regarding the fact that it is possible to implement an energy gap in graphene, it can be realized to show how nonzero effective mass of relativistic quasiparticles influences the electron dynamics in gapped graphene interacted with an ultrashort laser field. According to Eq. (13), the interband dipole matrix elements $D_x(\mathbf{k})$ and $D_y(\mathbf{k})$ are found to be complex functions and strongly depend on the electron wave vector $\mathbf{k}$. Their absolute value is singular at the Dirac points, K and K', in the corners of Brillouin zone, as shown in Figs. 2(a) and 2(b), where the energy gap causes to fall strongly from the height of sharp peaks. There is no coupling at the center of the Brillouin zone (Γ point). In Fig. 3, we plot the total CBP $N_{\mathrm{CB}}(t)$ as a function of time for various

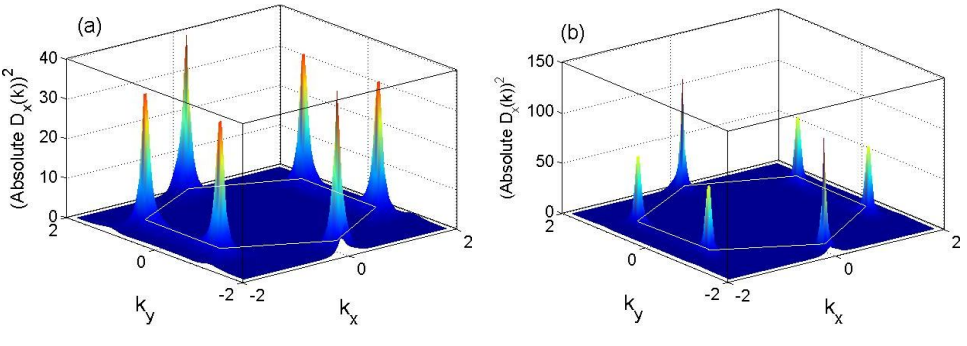

Fig. 2. (Color online) Plot of absolute of x-component of dipole matrix element as a function of wave vectors, (a) for energy gap $m = 0.5$ and (b) $m = 0.3$.

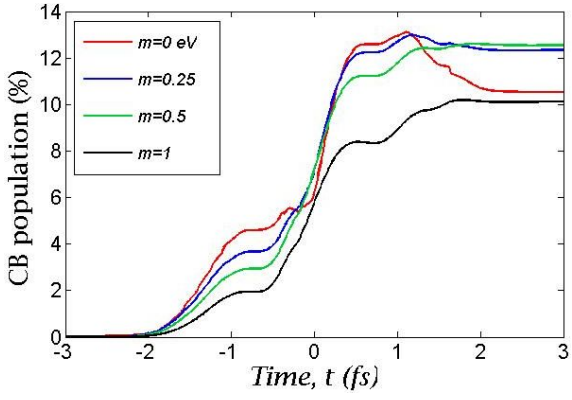

Fig. 3. (Color online) Population of the CB $N_{\mathrm{CB}}(t)$ as a function of time for different values of energy gap, which for all states we take $F_0 = 1$ $V/\text{Å}$ and $\theta = 0$.

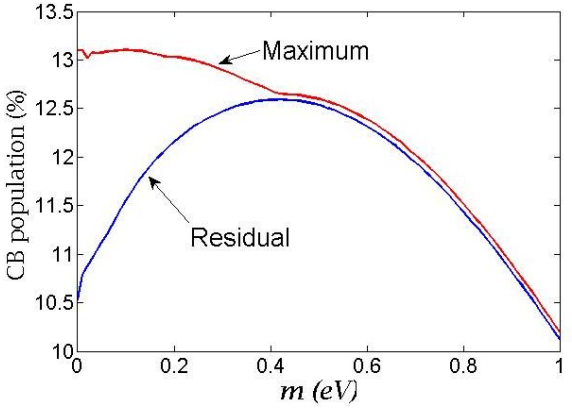

Fig. 4. (Color online) Curves of maximum and residual CBP as a function of bandgap.

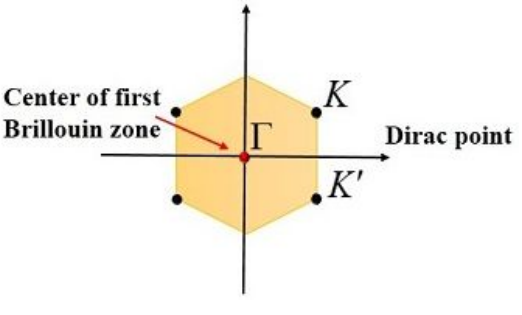

Fig. 5. (Color online) Dirac points in the reciprocal space in the first Brillouin zone.

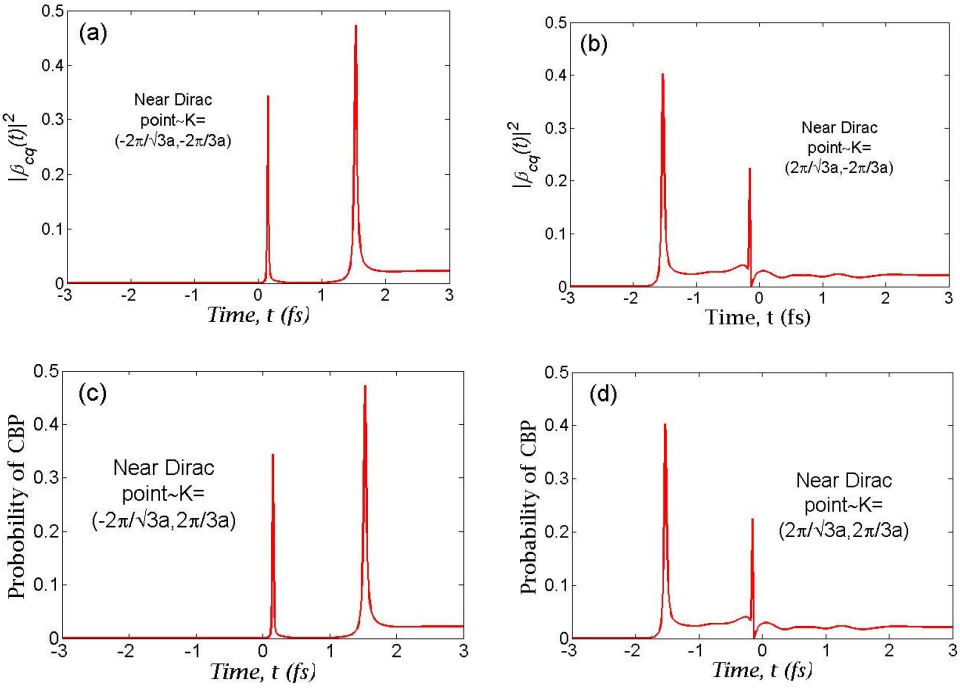

Fig. 6. (Color online) Plot of TP versus time for four Dirac K and K' points as shown in Fig. 5, for energy gap $m = 0.1$.

magnitudes of energy gap. Firstly, in agreeing with gapless graphene case, we obtain the irreversible feature of electron dynamics in strong electric field of an optical pulse when the pulse is over, and secondly, the residual of CBP is considerably even in large energy gaps. However, the energy gap in graphene causes to decrease a little the maximum of the CBP. To clarify the dependence of maximum and residual CBP on massive Dirac-like electrons is particularly presented in Fig. 4. We observe that, for low energy gaps, the maximum and residual CBP show fundamentally distinct behaviors, whereas they are equal and, of course, decrease rapidly for large energy gaps.

Further, we consider the transition probability (TP) $|\beta_{\mathrm{CB}}(t)|^2$ for four Dirac points (see Fig. 5) of Brillouin zone in terms of different energy gaps, for $m = 0.1$ in Fig. 6 and $m = 0.5$ in Fig. 7, respectively. We find unit probability with oscillating function of time in Dirac points for zero energy gap, which is not shown here. By applying an energy gap, the TP decreases, and a sharp peak of oscillating probability are found. Increasing energy gap causes more decrease in the TP. This feature is shown in Fig. 7. For right side of Dirac points in Fig. 5, the TP occurs for negative values of electric field of optical pulse and for left side, it happens once for positive electric field.

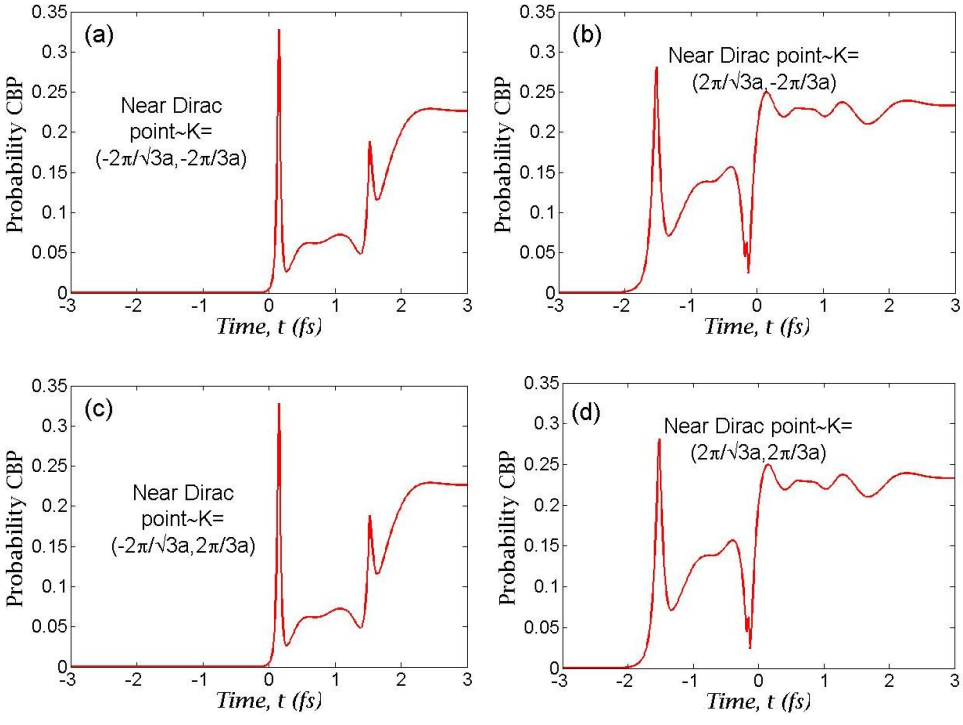

Fig. 7. (Color online) Plot of TP versus time for four Dirac K and K' points as shown in Fig. 5, for energy gap $m = 0.5$.

Using the acceleration theorem, we investigate the distribution of electrons around Dirac points K and K' during the pulse. In Fig. 8, we present nonuniform distribution of the CBP versus wave vectors in the reciprocal space in different times for nonzero energy gap in which the field strength is $F_0 = 1$ $V/\text{Å}$ and the polarization angle is $\theta = 0$. Regarding that the maximum peak of laser field is at $t = 0$, for $t \leq -0.75$ fs the field is negative, which accelerates the electrons to the right. Then the field changes its sign, the electrons start to move left. After the pulse end, the distribution becomes completely symmetric and interference fringes at the $k_x \approx 1$ Å^{-1} and -1 Å^{-1} Dirac points. We actually have considerable hot points in the reciprocal space for any magnitude of mass term. By increasing the gap, the area of hot points reduces due to the decreasing TP. The symmetric CB redistribution is found in Dirac points when the pulse end. However, recently Gierz *et al.*[37] have experimentally investigated the population inversion in the bilayer graphene (graphene with nonzero bandgap) in ultrashort laser field by the time- and angle-resolved photoemission spectroscopy. Due to the bandgap of bilayer graphene, the long-lived population inversion is demonstrated. These results can open up new opportunities for optoelectronics applications.

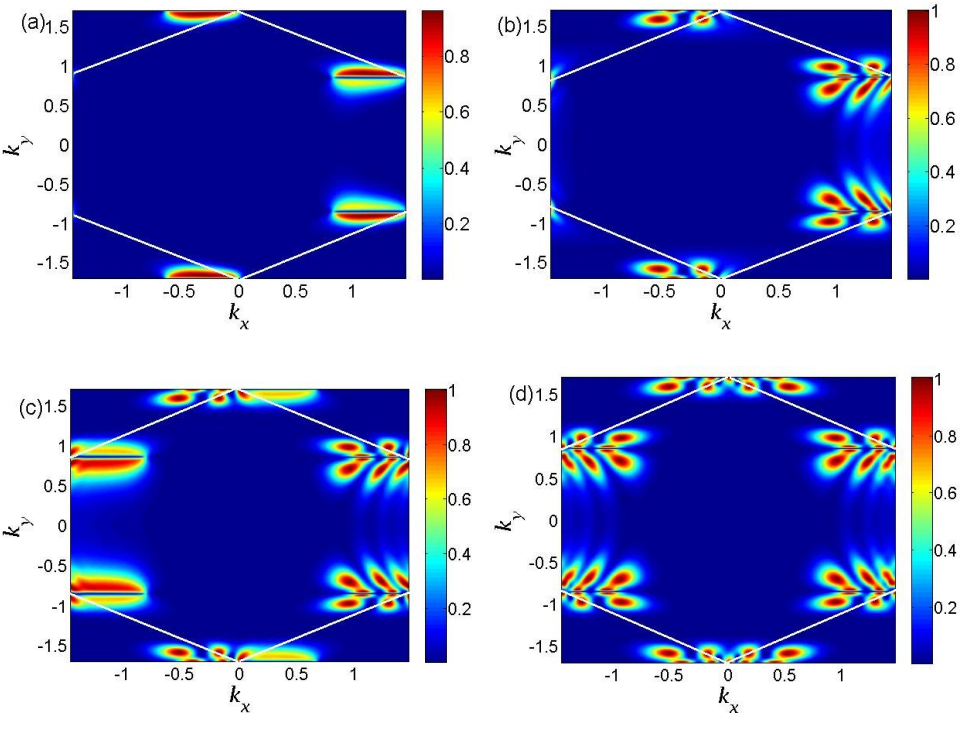

Fig. 8. (Color online) CB distribution of electrons at six Dirac points as a function of wave vector $\mathbf{k}$ for energy gap $m = 0.2$ in various times of optical pulse. Only the first Brillouin zone of the reciprocal space is shown, $F_0 = 1\ V/\text{Å}$ and $\theta = 0$. (a) The time is $t = -0.75$ fs, (b) $t = 0$, (c) for $t = 0.75$ fs and (d) in $t = 2.25$ fs.

4. Conclusion

In summary, in this paper, we have studied the transition of electrons from VB to the CB in graphene with nonzero bandgap (in fact, more real graphene). The relativistic massive Dirac electrons interact with an ultrashort (one optical oscillation) and strong ($\approx 1\ V/\text{Å}$) optical pulse. The electron dynamics of system was considered to be in coherent case due to no electron scattering. The effect of bandgap on the energy dispersion and correspondingly on Fermi wave vectors in graphene has been considered in the resulting transferred CBP and TP. Dipole matrix element of system has been found to be a complex function in x- and y-components. The numerical calculations of total transition rate for all Dirac points in first Brillouin zone in reciprocal space have shown a weak dependence of CBP on the bandgap parameter for $0 \leq m \leq 0.6$. Due to the singularity of dipole matrix element in reciprocal space, the existence of an energy gap results in an irreversible electron dynamics and nonuniform distribution of the CBP, which is in contrast with insulators. Moreover, in recent works,[38,39] the new effect of spin–orbit coupling in the single layer graphene on a single crystal film of a ferrimagnetic insulator have

been reported. It should be investigated as a future work the interaction of the proximity-induced ferromagnetic graphene with an optical pulse, since opening an energy gap can be realized by the magnetization vector.

Acknowledgment

The authors would greatly thank the anonymous reviewers for useful comments, which have helped us in improving this paper.

References

1. K. S. Novoselov *et al.*, *Science* **306**, 666 (2004).
2. A. H. Castro Neto *et al.*, *Rev. Mod. Phys.* **81**, 109 (2009).
3. C. Berger *et al.*, *J. Phys. Chem. B* **108**, 19912 (2004).
4. A. K. Geim and K. S. Novoselov, *Nature Mater.* **6**, 183 (2007).
5. X. Du *et al.*, *Nat. Nanotechnol.* **3**, 491 (2008).
6. K. I. Bolotin *et al.*, *Solid State Commun.* **146**, 351 (2008).
7. R. Balog *et al.*, *Nature Mater.* **9**, 315 (2010).
8. S. Y. Zhou *et al.*, *Nature Mater.* **6**, 770 (2007).
9. F. Varchon *et al.*, *Phys. Rev. Lett.* **99**, 126805 (2007).
10. I. Zanella *et al.*, *Phys. Rev. B* **77**, 073404 (2008).
11. R. M. Riberio *et al.*, *Phys. Rev. B* **78**, 075442 (2008).
12. G. Giovannetti *et al.*, *Phys. Rev. B* **76**, 073103 (2007).
13. E. V. Castro *et al.*, *Phys. Rev. Lett.* **99**, 216802 (2007).
14. T. G. Pedersen *et al.*, *Phys. Rev. Lett.* **100**, 136804 (2008).
15. T. G. Pedersen *et al.*, *Phys. Rev. B* **77**, 245431 (2008).
16. V. M. Pereira, A. H. Castro Neto and N. M. R. Peres, *Phys. Rev. B* **80**, 045401 (2009).
17. M. Gertsvolf *et al.*, *J. Phys. B* **43**, 131002 (2010).
18. A. V. Mitrofanov *et al.*, *Phys. Rev. Lett.* **106**, 147401 (2011).
19. M. Lenzner *et al.*, *Phys. Rev. Lett.* **80**, 4076 (1998).
20. M. Kruger, M. Schenk and P. Hommelhoff, *Nature* **475**, 78 (2011).
21. S. Ghimire *et al.*, *Nat. Phys.* **7**, 138 (2011).
22. M. Durach *et al.*, *Phys. Rev. Lett.* **105**, 086803 (2010).
23. L. Miaja-Avila *et al.*, *Phys. Rev. Lett.* **97**, 113604 (2006).
24. A. Schiffrin *et al.*, *Nature* **493**, 70 (2012).
25. M. Schultze *et al.*, *Nature* **493**, 75 (2012).
26. V. Apalkov and M. I. Stockman, *Phys. Rev. B* **86**, 165118 (2012).
27. V. Apalkov and M. I. Stockman, *Phys. Rev. B* **88**, 245438 (2013).
28. H. K. Kelardeh, V. Apalkov and M. I. Stockman, *Phys. Rev. B* **91**, 045439 (2015).
29. T. G. Pedersen, A.-P. Jauho and K. Pedersen, *Phys. Rev. B* **79**, 113406 (2009).
30. E. H. Hwang and S. Das Sarma, *Phys. Rev. B* **77**, 195412 (2008).
31. M. Breusing *et al.*, *Phys. Rev. B* **83**, 153410 (2011).
32. E. Malic *et al.*, *Phys. Rev. B* **84**, 205406 (2011).
33. D. Brida *et al.*, *Nat. Commun.* **4**, 1987 (2013).
34. I. Gierz *et al.*, *Nature Mater.* **12**, 1119 (2013).
35. A. Tomadin *et al.*, *Phys. Rev. B* **88**, 035430 (2013).
36. W. V. Houston, *Phys. Rev.* **57**, 184 (1940).
37. I. Gierz, M. Mitrano *et al.*, *J. Phys., Condens. Matter* **27**, 164204 (2015).
38. J. B. S. Mendes *et al.*, *Phys. Rev. Lett.* **115**, 226601 (2015).
39. Z. Wang *et al.*, *Phys. Rev. Lett.* **114**, 016603 (2015).